

# EVALUATION OF PAROTID GLAND TUMORS WITH MULTI-PHASE DYNAMIC HELICAL CT

A.Yusuf ÖNER, Gonca ERBAŞ, Serap GÜLTEKİN, Mehmet ARAÇ

## ABSTRACT

**Purpose:** To perform multi-phase dynamic helical computed tomography (CT) in patients with parotid gland tumors and to describe their enhancement characteristics.

**Materials and Methods:** A total of 19 patients were enrolled in this study. Multi-phase axial CT images were obtained before and 30, 90, 180, and 360 s after the contrast material injection. A late enhanced axial image was also obtained 25 min after the contrast material injection. The images were evaluated by two radiologists for lesion enhancement degree and pattern. For quantitative assessment density numbers measured in the early (30 s delay) and delayed (25 min delay) phases were compared. The tumoral enhancement ratio (ER) was also calculated by using the function  $ER = \text{Subscript}/\text{CTlate}$ . The histopathologic diagnosis was confirmed at surgical resection in all patients.

**Results:** There were twelve pleomorphic adenomas, five malignant tumors, and two Warthin tumors. At visual assessment five pleomorphic adenomas, one Warthin tumor and two malignant tumors showed homogeneous enhancement in the early phase. Heterogeneous enhancement with intratumoral low attenuation was seen in two pleomorphic adenomas, one Warthin tumor, and three malignant tumors. In early phase scans tumoral mean CT numbers were highest for the Warthin tumor. Pleomorphic adenomas and malignant tumors showed a slower contrast enhancement pattern. In delayed phase scans mean CT numbers were highest for pleomorphic adenomas. The resultant ER was highest for the Warthin tumor.

**Conclusion:** Multi-phase helical CT showed a pattern of strong enhancement in early phase scanning with a decrease in the delayed phase for the Warthin tumor. Although all non-Warthin parotid tumors showed a slower enhancement pattern, an increase in enhancement in delayed phase images might be suggestive of a pleomorphic adenoma. These enhancement patterns can be helpful in the differential diagnosis of parotid gland tumors.

**Key Words:** Parotis, Tumor, CT.

## PAROTIS BEZİ TÜMÖRLERİNİN ÇOK FAZLI DİNAMİK HELİKAL BT İLE DEĞERLENDİRİLMESİ

### ÖZ

**Amaç:** Kontrastlı multifaz dinamik bilgisayarlı tomografi ile parotis kitlelerinin kontrastlanma paternlerinin belirlenmesi ve cerrahi öncesi histopatolojik ayırıcı taniya katkısının araştırılması.

**Gereç ve Yöntem:** Parotis kitlesi olan toplam 19 hasta çalışmaya dahil edildi. Kontrast madde enjeksiyonu öncesinde ve sonrasında 30, 90, 180, 360 saniyeler ve 25 dakikada aksiyel planda BT görüntüleri elde edildi. Her hasta için elde olunan görüntü setleri iki farklı radyolog tarafından lezyonun kontrastlanma derecesi ve paterni açısından görsel olarak değerlendirildi. Kantitatif değerlendirme için lezyonların erken (30. saniye) ve geç evre (25 dakika) kontrastlı görüntülerdeki atenuasyon değerleri (AD) ölçülerek tümöral kontrastlanma oranı (KO)  $KO = \text{ADerken}/\text{ADgeç}$  formülü kullanılarak hesaplandı. Tüm hastalar cerrahi rezeksiyon sonrası kesin histopatolojik tanı aldı.

**Bulgular:** Çalışmaya dahil edilen hastaların on ikisi pleomorfik adenom (PA), beşi malign epitelial tümör (MET) ve ikisi Whartin tümörü (WT) tanısı aldı. 5 PA, 1 WT ve 2 MET erken fazda homojen kontrastlanma gösterdi. 7 PA, 1 WT ve 3 MET ise intratümoral düşük atenuasyon alanları içeren heterojen kontrastlanma paterni gösterdi. WT erken fazda yüksek kontrast tutarak takip eden fazlarda hızla bıraktığı izlendi. PA ve MET ise yavaş kontrastlanma paterni gösterdi. Ancak geç fazda PA'nın MET'ye göre daha yüksek kontrast tutulumu gösterdiği tespit edildi. KO değerlendirildiğinde en yüksek oran WT için hesaplandı.

**Sonuç:** Multifaz dinamik BT ile WT'de saptanan erken kontrast tutulumu parotis kitlelerinin preoperatif ayırıcı tanısında faydalı olabilecek bir bulgudur. MET ve PA benzer kontrastlanma paternlerine sahip olmakla birlikte, geç fazda PA'ların daha yüksek kontrast tutulumu göstermeleri ayırıcılarında yardımcı bir bulgu olarak kullanılabilir.

**Anahtar Kelimeler:** Parotis, Tümör, BT.

## INTRODUCTION

The surgical procedure chosen for salivary gland tumors is strongly influenced by their location and histologic type. Benign tumors are treated by local excision or superficial parotidectomy, whereas a more aggressive resection is chosen for malignant tumors.<sup>1-3</sup> Computed tomography (CT) and magnetic resonance imaging (MRI) are both commonly used in the preoperative evaluation of salivary gland masses. MRI findings of parotid tumors have previously been described and showed a good correlation between dynamic contrast enhancement pattern and histopathologic findings.<sup>5-6</sup> On CT, although an irregular tumor margin and infiltration suggest malignancy, there is considerable overlap among malignant and benign masses. There are few reports indicating the use of a two-phase dynamic helical CT in their characterization.<sup>7</sup> Thus the purpose of our study was to perform multi-phase dynamic helical CT in patients with parotid gland tumors and describe their enhancement characteristics.

## MATERIALS AND METHODS

Nineteen patients (ten male, nine female patients; age range, 32-66 years; mean age, 48 years) with a parotid mass, referred for presurgical evaluation between March 2000 and November 2002, were included in this study. The histopathologic diagnosis was confirmed after surgical resection in all patients. Written informed consent was obtained from each patient for this study.

All examinations were performed with a helical CT scanner (HiSpeed Advantage; GE Medical Systems, Milwaukee, WI, USA) capable of a 1 s gantry rotation time. A total of 90 mL of contrast agent was administered into an antecubital vein at a rate of 3 mL/s using a power injector. Multi-phase axial CT images were obtained before and 30, 90, 180, and 360 s after the contrast material injection. A late enhanced axial image was also obtained 25 min after the contrast material injection. For early contrast-enhanced images obtained with a delay of 30 s, the scanning began at the skull base and continued toward the thoracic inlet. For the non-enhanced and delayed-enhanced images the scanning range was limited to the parotid gland. Helical images were obtained with a 5 mm collimation 5 mm/s table speed, 120 kVp, and 80 mAs. From the volumetric data, contiguous transverse images were reconstructed at 5-mm intervals.

The images were transferred to a workstation and reviewed by two radiologists at one sitting. The radiologists evaluated image sets of a patient side by side at the same time and reached a consensus. The degree of lesion enhancement was graded as no enhancement, trace enhancement, moderate enhancement, or intense enhancement. The lesion enhancement pattern was visually assessed at each phase and classified as heterogeneous, hetero-

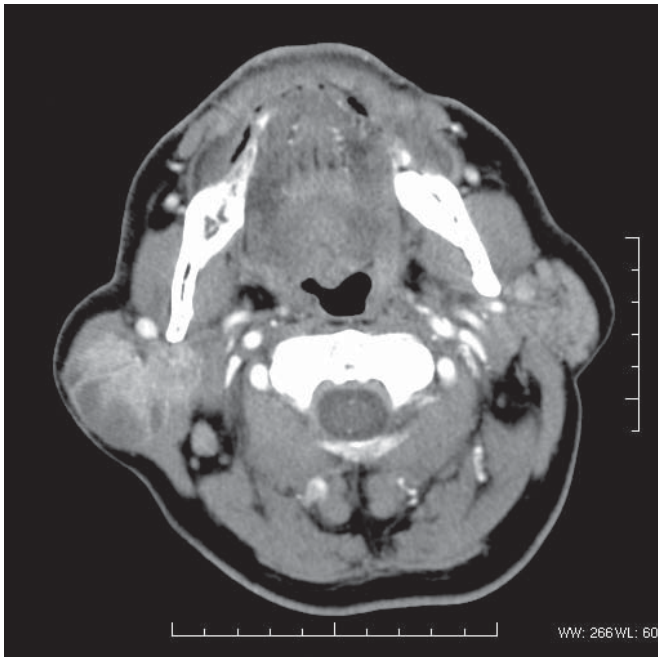


**Figure 1a:** Axial CT images acquired with a delay of 30 seconds (a) and 25 minutes (b) following contrast material injection of a 56 year-old man with Warthin tumor. The tumor shows a heterogeneous pattern of enhancement at early phase. Time-attenuation curve (c) for the same lesion depicts an early peak of enhancement with a high washout.

geneous enhancement with intratumoral low attenuation, or homogeneous. For quantitative assessment, density numbers in Hounsfield units (HU) of the lesions were recorded at each phase by means of the largest possible circular region of interest (ROI). When choosing the ROI, care was taken to exclude any cystic or necrotic areas. Density numbers measured in the early (30 s delay) and delayed (25 min delay) phase were compared. A plot representing the time-attenuation curve was constructed for each lesion. The tumoral enhancement ratio (ER) was calculated by using the function  $ER = \frac{\text{Subscript}}{\text{CTlate}}$ , where Subscript is the density number measured at 30 s delay, and CTlate is the density number measured at 25 min delay in Hounsfield units.

## RESULTS

There were twelve pleomorphic adenomas, five malignant tumors and two Warthin tumors. The size of lesions ranged between 14 and 52 mm (mean, 28 mm). In the visual assessment five pleomorphic adenomas, one Warthin tumor, and two malignant tumors showed homogeneous enhancement in the early phase. Heterogeneous enhancement with intratumoral low attenuation was seen in two pleomorphic adenomas, one Warthin tumor, and three malignant tumors. Five pleomorphic adenomas showed heterogeneous enhancement.

In the quantitative assessment, tumoral mean density numbers in early phase scans were highest for the Warthin tumor ( $105 \pm 16$  HU), followed by malignant tumors ( $83 \pm 19$  HU), and pleomorphic adenomas ( $69 \pm 14$  HU). In delayed phase scans,

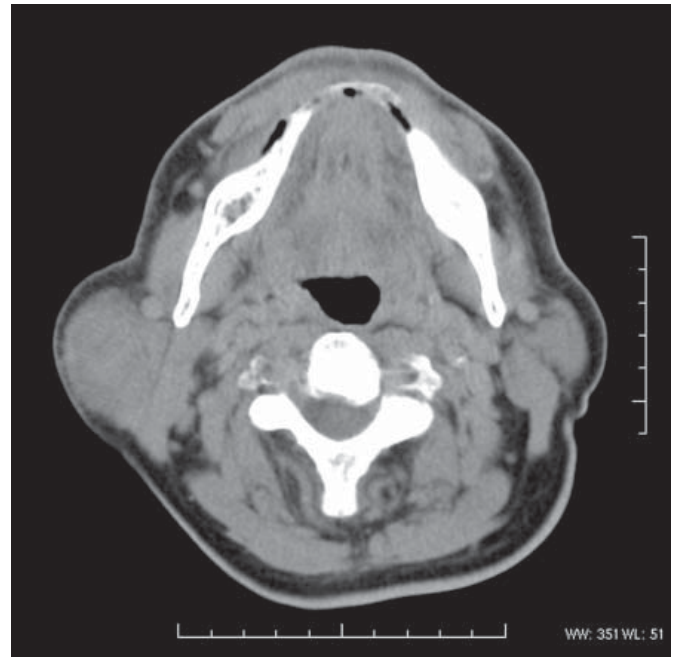


**Figure 1b:** Axial CT images acquired with a delay of 30 seconds (a) and 25 minutes (b) following contrast material injection of a 48 year-old woman with malignant tumor of the left parotid gland. The tumor shows a heterogeneous enhancement with intratumoral low attenuation at the early phase. Time-attenuation curve (c) for the same lesion depict an rapid enhancement with a slower washout.

tumoral mean density numbers were highest for pleomorphic adenomas, followed by malignant tumors, and the Warthin tumor (Table 1). The resultant ER was highest for the Warthin tumor. The number of patients included for each category was too few to statistically evaluate the relationship between the density numbers and the pathological diagnosis. The results are summarized in table 1.

## DISCUSSION

Preoperative differentiation between benign and malignant parotid tumors is important for adequate surgical planning and for the tumor prognosis. Aspiration cytology performed prior

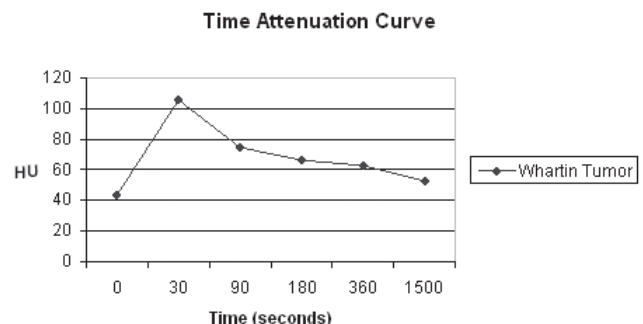


**Figure 1c:** Axial CT images acquired with a delay of 30 seconds (a) and 25 minutes (b) following contrast material injection of a 45 year-old man with pleomorphic adenoma. The tumor shows a homogeneous pattern of enhancement at early phase. Time-attenuation curve (c) for the same lesion depict an moderate enhancement with a slow washout.

**Table 1:** Enhancement ratio, and early and delayed phase density numbers of parotid gland tumors on multi-phase CT scan.

	Early Phase Density Number (HU)	Delayed Phase Density Number (HU)	ER
Warthin Tumor	105±16	53±17	1.98
Malignant Tumor	83±19	58±15	1.43
Pleomorphic Adenoma	69±14	66±13	1.05

Note.- Data are mean±standard deviation. HU: Hounsfield Units ER: Enhancement Ratio

to surgery is sometimes inconclusive due to insufficient samples, small tumor size, or a tumor located in the deep lobe of the parotid gland.<sup>8</sup> A more aggressive surgical procedure is performed to treat malignant tumors, which causes more frequent postoperative complications, such as facial nerve palsy. Therefore, predicting whether a parotid gland tumor is benign or malignant based on preoperative imaging findings is not only crucial in determining the surgical approach, but also in obtaining the patient's consent to undergo major neck surgery, which may eventually include sacrificing the facial nerve.

Static MRI findings of parotid gland tumors, with irregular tumor margin, heterogeneous signal intensity, tumor infiltration, and low T2 signal intensity indicating a possible malignant characteristic, have been previously reported.<sup>6,9,10</sup> In a recent study<sup>2</sup> enhancement patterns and corresponding time-intensity curves of salivary gland tumors were described by means of a dynamic MRI protocol. In that study, Yabuuchi et al. concluded that gadolinium-enhanced dynamic MRI can be useful in predicting histopathological tumor type.<sup>2</sup>

Compared with MRI, CT characteristics of parotid gland tumors have been less rigorously evaluated in the literature. Although irregular tumor margin and infiltration into adjacent structures suggest malignancy similarly to MRI, a malignant tumor may mimic benign tumors on conventional CT, with considerable overlap among various benign parotid gland pathologies.<sup>7</sup> Nowadays, with faster scanners, improved imaging times are possible, enabling the performance of multiphase contrast-enhanced CT studies. Lev et al.<sup>11</sup> evaluated delayed CT enhancement patterns of parotid pleomorphic adenomas. They reported that pleomorphic adenomas showed an increased degree of contrast enhancement on delayed scans. Choi et al. investigated the enhancement patterns of salivary gland tumors with two-phase dynamic helical CT in 64 patients.<sup>7</sup> They acquired axial images with scanning delays of 30 and 120 s. In 52 of 64 patients they also acquired late time images with a non-standard delay (6-25 min) after the contrast material injection. They reported that the two-phase helical CT showed a pattern of delayed enhancement in pleomorphic adenomas and a pattern of strong enhancement in early phase scanning with a decrease in the delayed phase in Warthin tumors. However, variable scanning delays used in the delayed images limited the accurate assessment of late tumoral enhancement. The protocol, consisting of two-phase acquisition, failed to provide sufficient data for the reconstruction of time-attenuation curves for each tumor type and this constituted a second limitation of their study.

In our study, the use of a multiple phase imaging protocol including late imaging 25 min after the contrast injection enabled us to determine time-attenuation curves and to accurately assess delayed tumoral enhancement. Warthin tumors showed an early and strong enhancement, whereas both malignant tumors and pleomorphic adenomas exhibited a slower enhancement pattern. Density numbers measured on delayed phase images were higher for pleomorphic adenomas. This finding is consistent with those obtained using dynamic MRI, which reported a peak signal intensity at 30 s following contrast injection for Warthin tumors and a gradual increase in signal intensity for up to 5 min for pleomorphic adenomas.<sup>2,12</sup> The time-attenuation curves obtained in our study were consistent with the time intensity curves of previous dynamic contrast enhanced MRI studies.<sup>2</sup>

The tumoral enhancement pattern is greatly influenced by tumor vascularity, histopathologic cell type, and the histological stromal component. Warthin tumors consist of an epithelial, mostly oncocytic component with a lymphoid stroma, and have a great tendency to undergo cystic change. Pleomorphic adenomas on the other hand contain mixed epithelial and stromal elements. The stroma can show mucoid, chondroid, fascicular, and hyalin-fibrous differentiation.<sup>7</sup> Malignant tumors can also have cystic components or show necrosis. This histological diversity of parotid gland tumors is well reflected in the visual assessment findings of the above presented study. It has also been hypothesized that early tumoral enhancement is related to tumoral microvasculature, whereas delayed enhancement reflects the cellularity and stromal component of the tumor.<sup>2,13</sup> Warthin tumors are known to have rich microvasculature, which helps explain their early and intense enhancement pattern. Because Warthin tumors tend to undergo cystic changes, they have less cellularity and a smaller stromal component, and therefore fail to retain contrast material on delayed phase images. On the other hand, malignant tumors, in addition to their various amounts of microvasculature and possible cystic necrotic foci, contain a larger stroma, which in turn retains contrast media in the late phases. Although both pleomorphic adenomas and malignant tumors show cystic changes, the former have more abundant fibrous stroma, which accounts for their higher late phase enhancement.

A main limitation of our study is the small number of patients included. Measured ERs were higher for Warthin tumors, followed by malignant tumors and pleomorphic adenomas. These findings correlate well with previous reports, but the numbers of Warthin and malignant tumors included in this

study are too small for statistical analysis or to allow us set a value for lesion characterization. Therefore, further studies with larger number of patients including different types of parotid tumors are needed.

In conclusion, multi-phase helical CT showed a pattern of strong enhancement in early phase scanning with a decrease in the delayed phase for Warthin tumors. Although all non-Warthin parotid tumors showed a slower enhancement pattern, an increase in enhancement in delayed phase images might be suggestive of a pleomorphic adenoma. These enhancement patterns can be helpful in the differential diagnosis of parotid gland tumors.

*Correspondence Adres*

*A. Yusuf Oner*

*Gazi University School of Medicine*

*Department of Radiology 06510, Besevler-Ankara Turkey*

*Telephone: 0 312 202 5163*

*Fax: 0 312 266 16 89*

*E-mail: yusuf@tr.net*

## REFERENCES

1. Yu, G.Y., D.Q. Ma, X.B. Liu, M.Y. Zhang, Q. Zhang, Local excision of the parotid gland in the treatment of Warthin's tumour. *Br J Oral Maxillofac Surg*, 1998. 36(3): p. 186-189.
2. Yabuuchi, H., T. Fukuya, T. Tajima, Y. Hachitanda, K. Tomita, M. Koga, Salivary gland tumors: diagnostic value of gadolinium-enhanced dynamic MR imaging with histopathologic correlation. *Radiology*, 2003. 226(2): p. 345-354.
3. Rehberg, E., H.G. Schroeder, O. Kleinsasser, [Surgery in benign parotid tumors: individually adapted or standardized radical interventions?]. *Laryngorhinootologie*, 1998. 77(5): p. 283-288.
4. Yousem, D.M., M.A. Kraut, A.A. Chalian, Major salivary gland imaging. *Radiology*, 2000. 216(1): p. 19-29.
5. Swartz, J.D., M.I. Rothman, F.I. Marlowe, A.S. Berger, MR imaging of parotid mass lesions: attempts at histopathologic differentiation. *J Comput Assist Tomogr*, 1989. 13(5): p. 789-796.
6. Joe, V.Q., P.L. Westesson, Tumors of the parotid gland: MR imaging characteristics of various histologic types. *AJR Am J Roentgenol*, 1994. 163(2): p. 433-438.
7. Choi, D.S., D.G. Na, H.S. Byun, Y.H. Ko, C.K. Kim, J.M. Cho, H.K. Lee, Salivary gland tumors: evaluation with two-phase helical CT. *Radiology*, 2000. 214(1): p. 231-236.
8. Takashima, S., F. Takayama, Q. Wang, M. Kurozumi, Y. Sekiyama, S. Sone, Parotid gland lesions: diagnosis of malignancy with MRI and flow cytometric DNA analysis and cytology in fine-needle aspiration biopsy. *Head Neck*, 1999. 21(1): p. 43-51.
9. Som, P.M., H.F. Biller, High-grade malignancies of the parotid gland: identification with MR imaging. *Radiology*, 1989. 173(3): p. 823-826.
10. Freling, N.J., W.M. Molenaar, A. Vermey, E.L. Mooyaart, A.K. Panders, A.A. Annyas, C.J. Thijn, Malignant parotid tumors: clinical use of MR imaging and histologic correlation. *Radiology*, 1992. 185(3): p. 691-696.
11. Lev, M.H., K. Khanduja, P.P. Morris, H.D. Curtin, Parotid pleomorphic adenomas: delayed CT enhancement. *AJNR Am J Neuroradiol*, 1998. 19(10): p. 1835-1839.
12. Takashima, S., Y. Noguchi, T. Okumura, H. Aruga, T. Kobayashi, Dynamic MR imaging in the head and neck. *Radiology*, 1993. 189(3): p. 813-821.
13. Murakami, T., H. Nakamura, K. Tsuda, T. Ishida, K. Tomoda, S. Hori, M. Monden, T. Kanai, K. Wakasa, M. Sakurai, et al., Contrast-enhanced MR imaging of intrahepatic cholangiocarcinoma: pathologic correlation study. *J Magn Reson Imaging*, 1995. 5(2): p. 165-170.